

Contaminants in Aquatic and Terrestrial Environments

**Dual-Element Isotope Analysis of Desphenylchloridazon
to Investigate its Environmental Fate in a Systematic
Field Study - A Long-Term Lysimeter Experiment**

Aileen Melsbach, Clara Torrentó, Violaine Ponsin, Jakov Bolotin, Laurence Lachat, Volker Prasuhn, Thomas B. Hofstetter, Daniel Hunkeler, and Martin Elsner

Environ. Sci. Technol., **Just Accepted Manuscript** • DOI: 10.1021/acs.est.9b04606 • Publication Date (Web): 02 Mar 2020

Downloaded from pubs.acs.org on March 5, 2020

Just Accepted

“Just Accepted” manuscripts have been peer-reviewed and accepted for publication. They are posted online prior to technical editing, formatting for publication and author proofing. The American Chemical Society provides “Just Accepted” as a service to the research community to expedite the dissemination of scientific material as soon as possible after acceptance. “Just Accepted” manuscripts appear in full in PDF format accompanied by an HTML abstract. “Just Accepted” manuscripts have been fully peer reviewed, but should not be considered the official version of record. They are citable by the Digital Object Identifier (DOI®). “Just Accepted” is an optional service offered to authors. Therefore, the “Just Accepted” Web site may not include all articles that will be published in the journal. After a manuscript is technically edited and formatted, it will be removed from the “Just Accepted” Web site and published as an ASAP article. Note that technical editing may introduce minor changes to the manuscript text and/or graphics which could affect content, and all legal disclaimers and ethical guidelines that apply to the journal pertain. ACS cannot be held responsible for errors or consequences arising from the use of information contained in these “Just Accepted” manuscripts.

1 Dual-Element Isotope Analysis of Desphenylchloridazon to Investigate its 2 Environmental Fate in a Systematic Field Study - A Long-Term Lysimeter 3 Experiment

4 Aileen Melsbach^{a,∇,§}, Clara Torrentó^{b,∇,†}, Violaine Ponsin^{b,¶}, Jakov Bolotin^c, Laurence Lachat^d, Volker
5 Prasuhn^e, Thomas B. Hofstetter^c, Daniel Hunkeler^b, Martin Elsner^{a,f,*}

6 ^aHelmholtz Zentrum München, Institute of Groundwater Ecology, 85764 Neuherberg, Germany

7 ^bCentre for Hydrogeology and Geothermics (CHYN), University of Neuchâtel, 2000 Neuchâtel, Switzerland

8 ^cEawag, Swiss Federal Institute of Aquatic Science and Technology, 8600 Dübendorf, Switzerland and Institute of
9 Biogeochemistry and Pollutant Dynamics, ETH Zürich, CH-8092 Zürich, Switzerland

10 ^dNeuchâtel Platform of Analytical Chemistry (NPAC), University of Neuchâtel, 2000 Neuchâtel, Switzerland

11 ^eAgroscope, Research Division, Agroecology and Environment, 8046 Zürich, Switzerland

12 ^fTechnical University of Munich, Chair of Analytical Chemistry and Water Chemistry, 81377 Munich, Germany

13

14 Abstract

15 Desphenylchloridazon (DPC), the main metabolite of the herbicide chloridazon (CLZ), is more water
16 soluble and persistent than CLZ and frequently detected in water bodies. When assessing DPC
17 transformation in the environment, results can be non-conclusive if based on concentration analysis
18 alone, because estimates may be confounded by simultaneous DPC formation from CLZ. This study
19 investigated the fate of DPC by combining concentration-based methods with compound-specific C and
20 N stable isotope analysis (CSIA). Additionally, DPC formation and transformation processes were
21 experimentally deconvolved in a dedicated lysimeter study considering three scenarios. First, surface
22 application of DPC enabled studying its degradation in the absence of CLZ. Here, CSIA provided evidence
23 of two distinct DPC transformation processes: one shows significant changes only in ¹³C/¹²C, whereas the
24 other involves changes in both ¹³C/¹²C and ¹⁵N/¹⁴N isotope ratios. Second, surface application of CLZ
25 mimicked a realistic field scenario showing that during DPC formation, ¹³C/¹²C ratios of DPC were depleted
26 in ¹³C relative to CLZ, while ¹⁵N/¹⁴N ratios remained constant. Finally, CLZ depth injection simulated
27 preferential flow and demonstrated the importance of the topsoil for retaining DPC. The combination of
28 the lysimeter study with CSIA enabled insights into DPC transformation in the field that are superior to
29 studies of concentration trends.

30

31 **Introduction**

32 Groundwater is one of the most important drinking water resources¹ and, therefore, constantly screened
33 for contaminants²⁻⁵. Due to their extensive application in agriculture, pesticides and their metabolites⁶ are
34 commonly detected in ground and surface water. A prominent example is desphenylchloridazon (DPC),
35 the main metabolite of the herbicide chloridazon (CLZ). CLZ is a selective systemic herbicide that is used
36 to control broad-leaved weeds in the agricultural production of swiss chard, red beet and sugar beet⁶⁻¹¹.
37 The metabolite DPC is a compound of concern as it is continuously formed from CLZ. The continuous input
38 of newly formed DPC makes it challenging to evaluate its environmental transformation from
39 concentration data over time. Detection of DPC has increasingly been reported exceeding concentrations
40 of 10 µg/L in natural water bodies^{6, 11-14}. DPC can be transported into ground and surface water by
41 precipitation events as it is water-soluble (490 mg/L), and has a lower tendency to bind to the soil
42 (Freundlich constant K_{foc} of 50 mL/g) than CLZ (K_{foc} of 199 mL/g). Additionally, DPC has a high leaching
43 potential, which is indicated by the groundwater ubiquity score (GUS) of 5.5, a parameter used to evaluate
44 pesticides for their potential to seep into the groundwater^{9, 15, 16}. Thus, there is great interest in the
45 question whether DPC can be subject to further transformation. The fate of DPC, however, is not well
46 understood yet^{2, 17, 18}. It is known that DPC is a persistent and polar compound. In soil, it can be further
47 transformed into methyl-desphenylchloridazon (MDPC, Figure S1)^{10, 12, 19, 20}. Whether there is a wider range
48 of degradation pathways, remains unclear.

49 Current attempts to quantify degradation of organic micropollutants are often based on metabolite-to-
50 parent-compound ratios. This is an analytical approach based on concentration measurements. It is
51 advantageous to quantify degradation even at low concentration ranges, and is simple to use²¹. However,
52 in case of DPC, which may be simultaneously formed while undergoing further transformation (Figure S1),
53 metabolite-to-parent ratios can lead to erroneous interpretations²². An additional confounding factor is a
54 different drainage-dependent re-mobilization of the parent compound and the metabolite due to
55 differences in their mobility. Thus, concentrations may fluctuate in a non-trivial manner making it difficult,
56 if not impossible, to inform about how much of the DPC has been transformed. Consequently, a
57 complementary method is needed to detect transformation if metabolite analysis alone is not conclusive.

58 Compound-specific stable isotope analysis (CSIA) allows to identify degradation processes by analyzing
59 variations of natural stable isotope abundances of different isotopic elements during (bio)degradation

60 and transformation of organic contaminants²³⁻²⁶. While CSIA of polar micropollutants has rarely been
61 performed at field scales²⁶, analytical methods for the analysis of carbon ($^{13}\text{C}/^{12}\text{C}$) and nitrogen ($^{15}\text{N}/^{14}\text{N}$)
62 isotope ratios of DPC have recently become available²⁷. So far, isotope studies of DPC have been carried
63 out neither in laboratory experiments nor in field applications, however. As illustrated in Figure S1, unique
64 insight on the formation and subsequent transformation of DPC can be expected. On the one hand, $^{13}\text{C}/^{12}\text{C}$
65 and $^{15}\text{N}/^{14}\text{N}$ ratios of DPC are expected to show the isotopic signature of the pyridazinone ring in the
66 precursor CLZ. When CLZ is transformed, its phenyl-ring is first oxidized and then cleaved off. Thus, any
67 isotope effect-induced changes in $^{13}\text{C}/^{12}\text{C}$ and $^{15}\text{N}/^{14}\text{N}$ ratios will be manifested in the molecular average
68 of CLZ and in the oxidized phenyl-part that is cleaved off. In contrast, none of the molecular positions of
69 the pyridazinone-ring are involved in the reaction, meaning that only secondary kinetic isotope effects
70 occur so that the isotope ratios within the pyridazinone-ring remain mainly unaffected when they end up
71 in DPC (Figure S1). If, however, further transformation of DPC takes place, this process is expected to
72 result in pronounced changes in isotope ratios in DPC, because now, carbon and nitrogen atoms are
73 directly involved (primary isotope effect). This would lead to carbon and nitrogen isotope fractionation in
74 DPC giving a strong indication of further DPC transformation²⁸. CSIA of DPC, therefore, holds promise to
75 identify both processes, formation of DPC from CLZ, as well as independent further transformation of DPC.
76 According to the current mechanistic picture, DPC is only formed from CLZ and transformed through N-
77 methylation^{19, 20, 29}. Thus, the combined analysis of carbon and nitrogen isotope ratios of DPC may offer
78 new insights into its fate in soil leachate.

79 Evidence from CSIA may be inconclusive, however, if physical processes (e.g., multiple sorption-
80 desorption steps, dissolution from non-aqueous phase, volatilization/diffusion, dispersion) or the
81 heterogeneity of the system, the soil in this case, affect degradation-induced changes in isotope ratios.
82 For example, a freshly dissolved compound, which has not been transformed yet, can mix with water
83 containing the contaminant that has already undergone varying degrees of degradation and thus isotope
84 fractionation³⁰⁻³². Consequently, the transformation-induced isotope ratios in the degraded fraction might
85 not be discernible any longer^{33, 34}. When applying CSIA to a field site either for the interpretation of a
86 compound's environmental fate or to monitor the success of remediation processes, it is therefore
87 suggested to combine it with complementary approaches in order to obtain as many lines of evidence as
88 possible^{30, 35, 36}.

89 Thus, the aim of this study was to explore different complementary and innovative approaches for
90 assessing the environmental long-term fate of DPC in drainage water after agricultural application over a

91 period of 3 years. To that end, we combined concentration measurements with the analysis of carbon and
92 nitrogen isotope ratios in a comprehensive and systematic study in a well-characterized model lysimeter
93 system. This lysimeter system mimics pesticides fate in natural soil environment under high control over
94 environmental and hydrological factors (i.e. soil type and humidity, precipitation levels, temperature,
95 evapotranspiration, etc.). In order to separate the relevant transport and transformation processes, these
96 complementary approaches were integrated into a dedicated experimental design where CLZ and DPC
97 were applied in three different scenarios (Figure S2): (i) DPC was applied to the lysimeter directly, without
98 the presence of CLZ, to investigate whether further DPC transformation is observable in drainage water
99 and whether this transformation is detectable from analyzing carbon and nitrogen isotope signatures of
100 DPC when interfering simultaneous formation of DPC can be excluded. (ii) The concurrent formation of
101 DPC from CLZ and potential DPC transformation were evaluated through surface application of CLZ to the
102 lysimeters. (iii) To simulate the preferential flow and to study whether DPC formation and transformation
103 is also occurring below the top soil, CLZ was injected below the root zone. For each scenario, these
104 complementary approaches were tested with two different soil types through a replication of the
105 lysimeter studies with moraine and gravel soil, respectively.

106

107 **Experimental / Methods**

108 **Experimental Set-up of Lysimeter Experiments.** For this study, the lysimeter facility from Agroscope was
109 used, located in Zurich-Reckenholz, Switzerland. The facility itself and the characteristics of the lysimeters
110 are described in detail by Torrentó et al.³⁷. Briefly, the site consisted of 12 gravitation lysimeters (L) (3.14-
111 m² surface area, 2.5 m depth, approximately 14 000 kg of soil in each) filled with two soil types
112 (gravel/moraine). Both soil types consisted of repacked Cambisol. Cambisols, widely and intensively used
113 as agricultural land, are among the most extensive soil types on earth, extending over about 11 % of the
114 global land surface³⁸. The soils used in this study differed in the B horizon and the draining properties of
115 the parent material, and thus they were expected to show a different extent of preferential flow³⁷. Gravel
116 soil was represented by well-drained sandy loamy Cambisol (L1-L6), while moraine soil consisted of a
117 poorly drained loamy Cambisol (L7-L12) (Table S1). Six of these lysimeters were used for this study (three
118 of each soil type). The lysimeters were planted in 2014 with corn (*Zea mays* L.) followed by sugar beet
119 (*Beta vulgaris* ssp. *vulgaris* var. *altissima* Doel) in 2015, with corn (*Zea mays* L.) again in 2016 and finally
120 with broccoli, Chinese cabbage, lettuce and leek in 2017. 3.0 kg/ha (0.96 g/lysimeter) of CLZ were applied

121 on the surface of two lysimeters (L4 and L8) simulating the scenario of pesticide application at the three-
122 to four-leaf stage in the field¹⁰. To simulate preferential transport through topsoil, two additional
123 lysimeters were used (L6 and L7), where 2.0 g of CLZ were injected in each lysimeter at a depth of 40 cm
124 at eleven injection points uniformly distributed over the area of each lysimeter by using a metal rod
125 connected to a gear pump through a Teflon tube. Additionally, 3.2 kg/ha (1.0 g/lysimeter) DPC was applied
126 on the surface of two lysimeters (L1 and L12). In addition to CLZ or DPC, the following tracers were applied
127 at the same time as the pesticides: uranine (1.3 kg/ha) and NaBr (500 kg/ha) to lysimeters L1 and L12,
128 uranine (1.3 kg/ha) to lysimeters L4 and L8, and uranine (0.4 g injected in each lysimeter) to lysimeters L6
129 and L7. Bromide was used as conservative tracer and uranine (K_{foc} of 120 mL/g) as a marker for preferential
130 leaching shortly after pesticide application³⁷. A detailed set-up is shown in the Supporting Information
131 (sections II.2 and II.3). Details about application methods can be found in Torrentó et al.³⁷. All lysimeters
132 were irrigated artificially and the seepage water was collected for analysis over a time period of 3 years
133 (Table S2).

134 **Concentration Measurements of CLZ, DPC and MDPC.** For concentration measurements of CLZ, DPC and
135 MDPC, an Ultimate[®] 3000 RS high-pressure liquid chromatography (HPLC) (Dionex, Thermo Fisher
136 Scientific, Waltham, MA, USA) coupled to a 4000-hybrid triple quadrupole-linear ion trap mass
137 spectrometer (QTRAP[®], ABSciex, Framingham, MA, USA) was used. Five microliters were injected on an
138 Acquity UPLC BEH Shield RP18 column (100 × 2.1 mm, 1.7 μm, Waters, Milford, MA, USA) maintained at
139 25 °C. The separation was performed at a flow rate of 0.4 mL/min using a binary mobile phase system
140 consisting of 0.05% formic acid in water (mobile phase A) and 0.05 % formic acid in acetonitrile (mobile
141 phase B) according to the following gradient program: 5-15 % phase B in 2 min, 15-100 % phase B in 4 min,
142 holding at 100 % phase B for 2 min, and re-equilibration at 2 % phase B for 6 min. Detection was
143 performed in electrospray positive ionization (ESI+) using the multiple reaction monitoring (MRM) mode
144 by monitoring both a quantifier (Q) and a qualifier (q) transition ion for each compound. Precursor and
145 fragment ions (m/z) were 222.1 and 104.0 (Q) or 77.0 (q) for CLZ, 146.0 and 117.0 (Q) or 66.0 (q) for DPC,
146 160.0 and 117.0 (Q) or 88.0 (q) for MDPC, and 227.0 and 108.0 (Q) or 81.0 (q) for CLZ-d₅, respectively
147 (Table S3). Quantification was performed using standard curves calculated from standard solutions of CLZ,
148 DPC and MDPC at 0.25, 0.5, 1, 3, 5 and 10 ng/mL, each containing deuterated CLZ-d₅ as internal standard
149 at a constant concentration of 2 ng/mL. The limits of quantification were 0.05 μg/L for CLZ, 0.4 μg/L for
150 DPC and 0.1 μg/L for M-DPC. For those drainage water samples with CLZ, DPC and MDPC concentrations
151 lower than 0.2 μg/L, solid-phase extraction (SPE) of 20-mL samples was performed using 6 mL cartridges
152 packed with 0.2 g of Bakerbond SDB-1 sorbent and 0.2 g of Septra ZT sorbent, as described by Torrentó et

153 al.³⁹. After SPE, the extracts were analyzed by UHPLC-QTOF-MS. The method is briefly described in the
154 Supporting Information (II.5.).

155 **Large Volume Solid-Phase Extraction.** For isotope analysis, all lysimeter samples were filtered through
156 0.7- μm glass fiber filters and were concentrated by SPE using the method described in Torrentó et al.³⁹,
157 as detailed in the Supporting Information (II.6.).

158 **Elemental Analyzer-Isotope Ratio Mass Spectrometry Measurement for Determination of Reference**
159 **Values.** Carbon and nitrogen isotope reference values of our in-house standards of CLZ, DPC and MDPC
160 were determined by elemental analysis – isotope ratio mass spectrometry (EA-IRMS) according to the
161 method of Meyer et al.⁴⁰. The system consisted of an EuroEA (Euro Vector, Milano, Italy) coupled with a
162 Finnigan MAT 253 IRMS via a FinniganTM ConFlow III interface (Thermo Fisher Scientific, Bremen,
163 Germany). For calibration, USG 40, USG 41 (L-glutamic acid) and IAEA 600 (caffeine), supplied by the
164 International Atomic Agency (IAEA), were used as organic reference materials.

165 Carbon ($\delta^{13}\text{C}$) and nitrogen ($\delta^{15}\text{N}$) isotope signatures are usually expressed using the Delta notation in per
166 mille as described in equation 1 and 2. There, the isotope ratios ($^{13}\text{C}/^{12}\text{C}_{\text{sample}}$ and $^{15}\text{N}/^{14}\text{N}_{\text{sample}}$) are stated
167 relative to the international references PeeDee Belemnite (V-PDB) for carbon and air for nitrogen.

$$\delta^{13}\text{C} = \frac{^{13}\text{C}/^{12}\text{C}_{\text{Sample}} - ^{13}\text{C}/^{12}\text{C}_{\text{Reference}}}{^{13}\text{C}/^{12}\text{C}_{\text{Reference}}} \quad (1)$$

168

$$\delta^{15}\text{N} = \frac{^{15}\text{N}/^{14}\text{N}_{\text{Sample}} - ^{15}\text{N}/^{14}\text{N}_{\text{Reference}}}{^{15}\text{N}/^{14}\text{N}_{\text{Reference}}} \quad (2)$$

169

170 **Carbon Isotope Analysis of DPC by LC- IRMS.** For carbon isotope analysis of DPC we applied the method
171 of Melsbach et al.²⁷. Briefly, 10 to 100 μL of SPE extracts reconstituted in ultrapure water were injected
172 into an LC-IRMS Dionex system consisting of an Ultimate 3000 HPLC pump and an Ultimate 3000
173 autosampler (Thermo Fisher Scientific) coupled via an LC-Isolink interface with a Delta V Advantage IRMS
174 (Thermo Fisher Scientific). Chromatography was accomplished using a Sentry guard column (3 μm ,
175 20 mm) and an Atlantis T3 column (3 μm , 100 mm, Waters) at a flow rate of 500 $\mu\text{L}/\text{min}$. Phosphoric acid
176 at pH 2 was chosen as mobile phase. The method was run isocratically at room temperature. The analytes
177 were converted by wet oxidation at a temperature of 99.9 $^{\circ}\text{C}$ after the separation unit. Thereto, 90 g/L

178 $\text{Na}_2\text{S}_2\text{O}_8$ and phosphoric acid (1.5 M H_3PO_4) were introduced at a flow rate of 30 $\mu\text{L}/\text{min}$. The vacuum
179 inside the IRMS was 2×10^{-6} mbar. Its ion source was set to an accelerating voltage of 3 kV and an electron
180 ionization energy of 124 eV. The isotope ratios were calibrated using our laboratory monitoring gas (CO_2),
181 which had previously been calibrated against the international standard RM8563 (CO_2), supplied by the
182 IAEA.

183 **Derivatization of DPC for Nitrogen Isotope Analysis.** Nitrogen isotope analysis was conducted using the
184 derivatization procedure proposed by Melsbach et al.²⁷. Briefly, DPC was methylated to MDPC by adding
185 an excess of greater than $160 n_{\text{analyte}}/n_{\text{TMSD}}$ (140 μL of a 2 M TMSD solution) into a vial containing a
186 standard or a SPE extract reconstituted in 1 mL methanol. The vial was crimped tightly before putting it
187 into a 70°C water bath for 2 h. For samples from lysimeters with CLZ depth injection, the volume of the
188 2 M TMSD solution added to the reconstituted SPE extracts was increased to 200 μL to ensure complete
189 derivatization, as concentrations of DPC were up to an order of a magnitude higher compared to the other
190 lysimeter samples. Afterwards, the solvent was evaporated to dryness. The sample was then reconstituted
191 in 50 μL acetone.

192 **Separation of Drainage Sample Fractions for Analysis of DPC and MDPC.** For drainage water samples
193 from the lysimeters where CLZ was applied on the surface and for which the ratio of DPC to naturally
194 formed MDPC was greater than 10 %, preparative HPLC was used prior to derivatization to isolate this
195 naturally formed MDPC and thus to avoid interferences in the isotopic signature of DPC when subjected
196 to methylation in the derivatization procedure. The method is briefly summarized in the Supporting
197 Information (II.7.)²⁷. Additionally, both DPC and MDPC fractions were used for $\delta^{15}\text{N}$ isotope analysis when
198 possible. For samples with an MDPC to DPC ratio <10 %, no preparative HPLC method was applied prior
199 to derivatization, as the influence of the isotope ratio of MDPC on the isotope ratio of derivatized DPC is
200 negligible and lies within the measurement error for nitrogen CSIA (± 1 ‰) of the developed ^{15}N GC-IRMS
201 method²⁷.

202 **Nitrogen Isotope Analysis of DPC and MDPC.** The method is described by Melsbach et al.²⁷ Briefly, a
203 TRACE GC Ultra gas chromatograph (Thermo Fisher Scientific, Milan, Italy) coupled with a Finnigan MAT
204 253 IRMS (Thermo Fisher Scientific, Bremen, Germany) was used. A Finnigan Combustion III interface
205 (Thermo Fisher Scientific) connected both instruments. The analytes were combusted at a temperature
206 of 1030 °C with a NiO tube/ CuO -NiO reactor (Thermo Fisher Scientific). The gas chromatograph contained
207 a DB-1701 column (30 m \times 0.25 mm \times 1 μm , J&W Scientific, Santa Clara, CA). Helium (grade 5.0) at a flow
208 rate of 1.4 mL/min was used as carrier gas. Injection was carried out with a GC Pal autosampler (CTC,

209 Zwingen, Switzerland). A sample volume ranging between 1 and 3 μL was injected into a splitless liner
210 (Thermo Fischer Scientific, Australia) at a temperature of 250 $^{\circ}\text{C}$. The GC oven was programmed to start
211 at a temperature of 100 $^{\circ}\text{C}$ (held for 1 min), ramped with 25 $^{\circ}\text{C}/\text{min}$ to 240 $^{\circ}\text{C}$, and with 10 $^{\circ}\text{C}/\text{min}$ to
212 280 $^{\circ}\text{C}$ (held for 5 min). The isotope ratios were calibrated using our laboratory monitoring gas (N_2), which
213 had previously been calibrated against the international standard NSVEC (N_2), supplied by the IAEA.

214 **Correction Procedure for Isotope Analysis.** Analogous to the correction procedure described by Melsbach
215 et al.²⁷, all samples and standards were measured in triplicate and their isotope ratios are reported as the
216 arithmetic means with their respective estimated standard deviations ($\pm \sigma$). In addition to the calibration
217 of the measurement gas, samples are bracketed within the sequences by in-house standards of DPC and
218 MDPC, whose isotopic signature had been determined with EA-IRMS (Table S4). Here, the principle of
219 identical treatment by Werner and Brand⁴¹ was applied to correct for trueness by identifying drifts and
220 off-sets, caused by different combustion efficiency. $\delta^{15}\text{N}$ correction was performed using MDPC
221 synthesized by LGC Standards GmbH, while an authentic DPC standard was used for $\delta^{13}\text{C}$ correction of the
222 LC-IRMS method.

223 **Concentration Measurement of CLZ and DPC from Soil Samples.** CLZ and DPC residues were measured
224 within the first soil layers (0 to 10 cm) approximately one year after herbicide/metabolite application. To
225 obtain a representative and homogenous sample, subsamples for soil analysis were collected in
226 quadruplets and combined afterwards. The total amount was at least 100 g soil per sample. Sample
227 extraction and analysis were carried out by Eurofins Sofia GmbH using LC-MS/MS.

228 **Statistical Analyses.** Pearson correlation analysis and one-way analyses of variance (ANOVA) tests were
229 performed to identify patterns and to measure the statistical significance of the relationship between
230 variables. ANOVA tests were performed to assess the differences between soil types and pesticide
231 application methods regarding total accumulated drainage, total DPC mass leached, maximum change of
232 carbon and nitrogen isotope signatures 900 days after pesticide application/injection. Separate Pearson
233 linear correlations were performed to evaluate the relationship between irrigation and drainage, between
234 soil humidity and drainage, between drainage and DPC mass leached, and between evapotranspiration
235 and DPC mass leached. All tests were performed using the statistical package Minitab 13.31 (Minitab Inc.,
236 State College, PA). All statistical differences were set to the $\alpha = 0.05$ significance level ($p \leq 0.05$).

237 **Results and Discussion**

238 **Water Dynamics.** Total accumulated drainage 900 days after CLZ or DPC application/injection was
239 between 488 to 656 mm for gravel soil and between 337 and 502 mm for moraine soil. In relation to the
240 water input, drainage represented 25-39 % and 18-27 % of the total irrigation, respectively. Increased
241 drainage coincided with periods of high irrigation intensity and high soil water content. A significant
242 positive correlation (Pearson's correlation coefficient – r – from 0.30 to 0.49, $p < 0.0001$) between
243 intensity of daily irrigation and daily drainage was observed for the six lysimeters. As detailed by Torrentó
244 et al.³⁷, who used the same lysimeters to assess the fate of the herbicide atrazine and its metabolites, soil
245 humidity data revealed that large irrigation events resulted in a greater contribution of preferential flow
246 to drainage, and that this effect was more significant for the moraine than for the gravel soil. A statistically
247 significant ($p < 0.05$) correlation was observed between soil humidity and drainage for both gravel and
248 moraine soil at all depths where capacitance sensors were installed (at 16, 36, 56, 76, and 96 cm for
249 moraine soil and at 11, 51, and 71 cm for gravel soil)³⁷. This correlation was stronger for moraine (r
250 between 0.15 and 0.22, except for one depth with $r = 0.08$) than for gravel soil (r between 0.06 and 0.16),
251 and is in accordance with the fact that fluctuations in the soil water content were smaller for the latter,
252 especially at greater depths³⁷. The total accumulated drainage after 900 days was influenced by the
253 application method (higher drainage for depth injection, $p = 0.331$) and by the soil type (higher for gravel
254 soil, $p = 0.426$). Large amounts of drainage from the gravel soil are probably a consequence of the higher
255 water permeability and low water content at field capacity of this soil³⁷.

256 The average monthly and annual irrigation, drainage, and evapotranspiration values for the lysimeters
257 used in this study are shown in Table S5. Annual evapotranspiration, estimated by the water balance
258 computation as explained by Torrentó et al.³⁷, was for the four years of study (2014 to 2017) higher for
259 moraine (315 to 633 mm) than for gravel soil (266 to 585 mm), although the effect was not statistically
260 significant ($p = 0.718$). A significant effect ($p = 0.002$) on annual evapotranspiration was however observed
261 for crop type: evapotranspiration was higher for sugar beet and corn than for broccoli, Chinese cabbage,
262 lettuce and leek. The effects of soil type and pesticide application method on evapotranspiration 900 days
263 after pesticide application were not statistically significant ($p = 0.093$ and $p = 0.579$, respectively). The
264 influence of the cover vegetation on drainage and pesticides fate was not assessed, since no significant
265 differences in the plants development were observed between lysimeters. For details, see Supporting
266 Information section III.2.

267 **Trends in Compound Concentrations after DPC Surface Application.** Neither CLZ, nor DPC had ever been
268 applied to any of the lysimeters prior that study so that trends for CLZ and DPC concentrations could be

269 uniquely attributed to our experimental design. Through application of the metabolite DPC to the surface
270 of the lysimeters, it was possible to investigate the fate of DPC separately, in the absence of CLZ and
271 without interference of constantly formed DPC. The breakthrough of DPC in the seepage water differed
272 between the soil types (Figure 1b). In the lysimeter with moraine soil (L12), concentrations changed more
273 rapidly in relation with drainage events than for gravel soil (L1). For gravel soil (L1), DPC was detected in
274 the drainage water for the first time after 137 days, while it broke through only 15 days after application
275 in moraine soil (L12). In these lysimeters, a positive correlation was observed between drainage and DPC
276 mass leached, being more significant for gravel ($r = 0.36$, $p = 0.029$) than for moraine soil ($r = 0.31$, $p =$
277 0.113). The observed dependency of the drainage response, and the analytes' concentration therein, on
278 the irrigation agrees with Torrentó et al.³⁷ for the fate of the herbicide atrazine and its metabolites in
279 these lysimeters. Table S6 summarizes the observed breakthrough parameters for each lysimeter. Two
280 main DPC concentration peaks were detected in the drainage water of these two lysimeters after
281 approximately 550 and 850 days (Figure 1e). They coincided with two intense irrigation events (November
282 2016 and September 2017, Table S2). In moraine soil (L12, 303 and 441 mm), less accumulated drainage
283 had occurred at peak concentration of DPC than in the gravel soil (L1, 458 and 852 mm). Concentrations
284 in the gravel soil were approximately one order of magnitude higher than in moraine soil. In contrast to
285 our previous study³⁷, no rapid breakthrough peak was observed shortly after application, neither for DPC
286 nor for uranine (Figure S4). Bromide mass recovery curves (Figure S5) showed an asymmetric sigmoidal
287 shape, which is characteristic for transport through a porous matrix with some retardation. Smoother
288 trends for DPC compared to the tracers indicate retardation by sorption and/or attenuation by
289 degradation. DPC leaching was therefore mainly driven by porous matrix flow, although intense irrigation
290 events resulted in a greater contribution of preferential flow. This was observed mainly in moraine soil.
291 For example, after 425 and 670 days, sharp increases in DPC concentrations were measured (Figure S4).
292 This might be a consequence of transport by preferential flow induced by intense irrigation events (July
293 2016 and March 2018, respectively, Table S2).

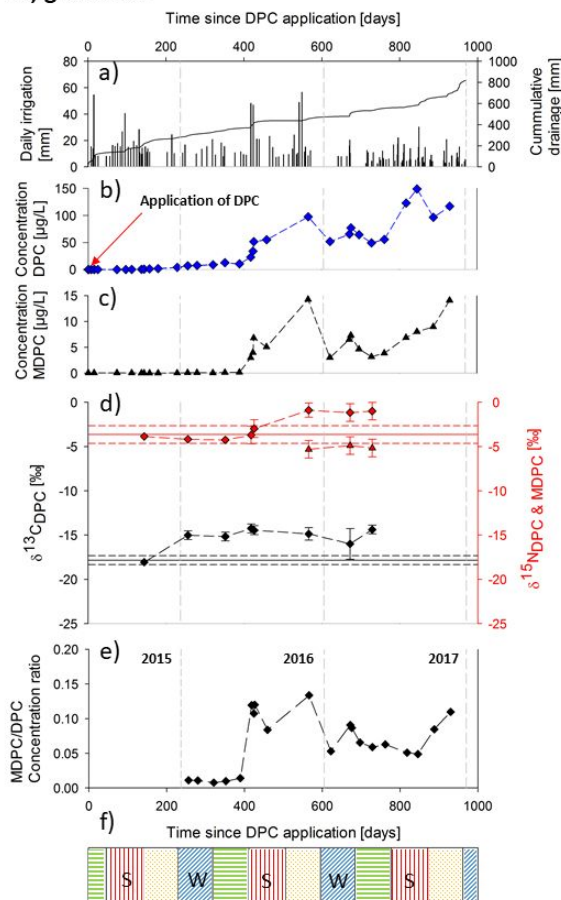
294 The transformation product of DPC, MDPC, was first detected after 256 days and 425 days for gravel and
295 moraine soil, respectively. At the end of the monitoring period (950 days after DPC application), 6.0 % of
296 the DPC mass was recovered in the drainage water of the gravel soil and only 0.3 % in the moraine soil
297 (details about the calculation of analyte recovery can be found in the Supporting Information section II.9).
298 MDPC accounted for 0.55 % and 0.06 % of the applied DPC, respectively. One year after application, a DPC
299 residue of approximately 3 % and 7 % of the applied DPC was quantified within the first soil layers (0 to
300 10 cm) of gravel and moraine soil, respectively (Table S7). Thus, an incomplete mass balance was

301 observed. Here, possible explanations might be: (i) sorption of DPC to lower soil layers within the root
302 zone, where further sampling was not possible without disturbing the lysimeter, (ii) the uptake and
303 metabolism of DPC by plants^{42,43}, and (iii) the presence of DPC-fulvic acid complexes, as their functional
304 groups can bind DPC. This has been demonstrated by Gatzweiler⁴⁴, who conducted lysimeter experiments
305 with ¹⁴C-labelled CLZ. Using thin-layer chromatography and analyzing the radioactivity, Gatzweiler⁴⁴
306 detected DPC in fulvic acid fractions verifying the existence of these DPC-fulvic acid complexes.
307 Nevertheless, the MDPC/DPC concentration ratio suggests that further DPC degradation to MDPC
308 occurred in both soils, mainly after 425 days. (As both DPC and MDPC have a similar GUS leaching
309 potential and show only minor differences in their mobility, no major retardation effect on the transport
310 of either compound is expected so that the use of metabolite-to-parent compound ratios appears justified
311 in this case)⁹. This further degradation agrees with the findings of Schuhmann et al.⁴² and the
312 environmental degradation pathway predicted by Roberts et al.¹⁹. This demonstrates that transformation
313 of DPC is occurring only slowly. For the moraine soil, a local maximum for the MDPC/DPC concentration
314 ratio was reached after 750 days (Figure 1, L12e). To obtain additional insight into DPC transformation,
315 we, therefore, evaluated the results from CSIA of the lysimeter experiment.

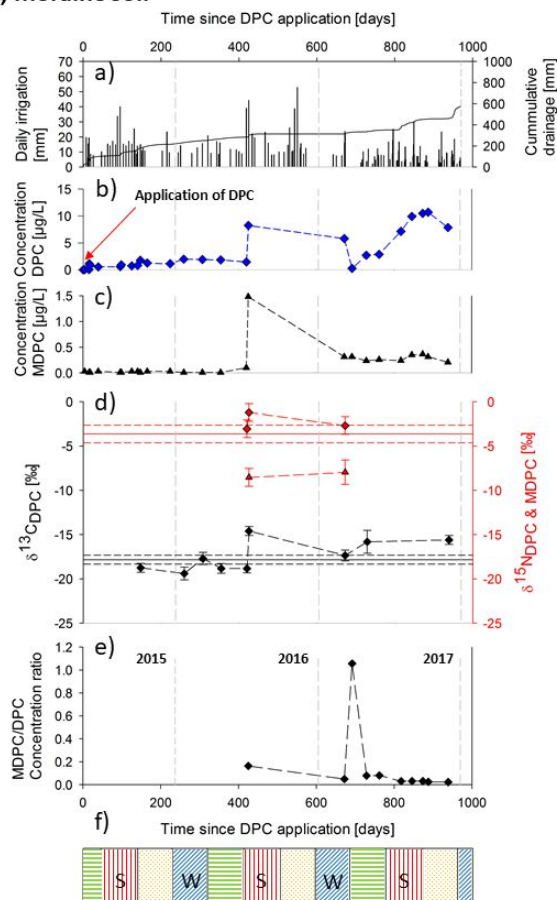
316 **Insights into DPC Transformation by Isotope Analysis of DPC from Surface Application.** Initially, the $\delta^{13}\text{C}$
317 and $\delta^{15}\text{N}$ values of the leached DPC were close to the original isotope signature of the applied DPC
318 (Figures 1, L1d and L12d). Over the course of the observation period carbon isotope signatures of DPC
319 showed significant enrichment in ¹³C ($\Delta\delta^{13}\text{C}_{\text{DPC}}$) of approximately +4 ‰ in both soil types. The heavy
320 irrigation event 672 days after DPC surface application (March 2017, Table S2) caused a new small DPC
321 breakthrough peak, in which DPC isotope values returned to the original isotopic composition, most likely
322 because new DPC was mobilized, which had not yet been subject to transformation. This effect was more
323 significant in moraine soil, where a greater contribution of preferential flow in response to this heavy
324 irrigation event was observed, resulting in a recovery of up to 20 % of the total mass of DPC leached in
325 the drainage water after the monitoring period. Additionally, significant changes of nitrogen isotope
326 signatures ($\Delta\delta^{15}\text{N}_{\text{DPC}}$) of +2 ‰ to +3 ‰ were observed – however, mainly in the gravel soil (L1).
327 Furthermore, these shifts were observed at a later time point than the enrichment in ¹³C, approximately
328 450 days after application. The fact that during the first 450 days DPC was only becoming enriched in ¹³C,
329 and then in both ¹³C and ¹⁵N, suggests that DPC was transformed by two distinct processes and that only
330 the latter one starting after 450 days involved a reaction of a nitrogen atom. The transition between the
331 two trends coincides with an increase in the MDPC/DPC concentration ratio (Figure 1, L1e). As there had
332 never been any application of CLZ or DPC to these lysimeters, the carbon and nitrogen isotope values of

333 DPC can be uniquely attributed to the substance applied in this study, and changes in these isotope
334 signatures are attributable to its further degradation. Interestingly, due to the high concentrations of
335 MDPC in the drainage water, it was possible to measure the $\delta^{15}\text{N}$ of formed MDPC after purification by
336 preparative HPLC (Tables S9 and S10). In both lysimeters, the $\delta^{15}\text{N}$ of MDPC was significantly more
337 negative (approximately by 4‰) compared to the $\delta^{15}\text{N}$ value of the DPC at that time (Figure 1d). Since
338 DPC contains three nitrogen atoms out of which only one is methylated, it can be estimated that the
339 methylation of DPC causes a nitrogen isotope effect of approximately $3 \times 4 \text{ ‰} = +12 \text{ ‰}$ at the reactive
340 atom. Our data for the DPC surface application show an enrichment in ^{13}C and, to a lesser extent, in ^{15}N
341 for DPC in both soils, which was significantly masked in the moraine soil due to the leaching of fresh DPC
342 after heavy irrigation events. Transformation extent can thus be underestimated. Here, transformation of
343 DPC may be easier to detect using the metabolite-to-parent concentration ratio, at least for the pathway
344 involving MDPC formation. On the other hand, using the metabolite-to-parent concentration ratio only to
345 investigate the transformation of DPC, the evidence of an additional transformation mechanism would
346 have remained undetected. Additionally, CSIA appears to be more robust as the integrated isotope signal,
347 which indicates degradation remains measurable, even if the metabolite might be subject to sorption or
348 further transformation.

L1, gravel soil



L12, moraine soil



349

350 **Figure 1.** Lysimeters with DPC application on surface (a single application in May 2015): L1 in gravel soil (left panels) and L12
 351 in moraine soil (right panels). a) Daily irrigation (black bars) and cumulative drainage (grey line); b-c) Concentration of DPC
 352 (blue diamonds) and MDPC (black triangles), note that different scales are used for both soil types; d) Carbon (black diamonds)
 353 and nitrogen (red diamonds) isotope ratios of DPC and nitrogen isotope values of MDPC (petrol triangles), error bars show the
 354 associated uncertainties ($\pm 0.5\text{‰}$ for carbon, $\pm 1.0\text{‰}$ for nitrogen isotope analysis; or when exceeding this uncertainty,
 355 standard deviations of triplicate measurements are given, EA isotope values of the applied DPC are shown as lines, whereas
 356 associated uncertainties ($\pm 0.5\text{‰}$ for carbon, $\pm 1.0\text{‰}$ for nitrogen isotope analysis) are shown as dashed lines in the
 357 corresponding color, respectively; e) metabolite-to-parent compound molar ratio of MDPC/DPC (black diamonds); f) season
 358 corresponding to the time since application – spring (green horizontal lines), summer (red vertical lines), autumn (yellow dots),
 359 winter (blue diagonal lines); the grey dashed lines repeated in each sub-figure represent the start of a new year.

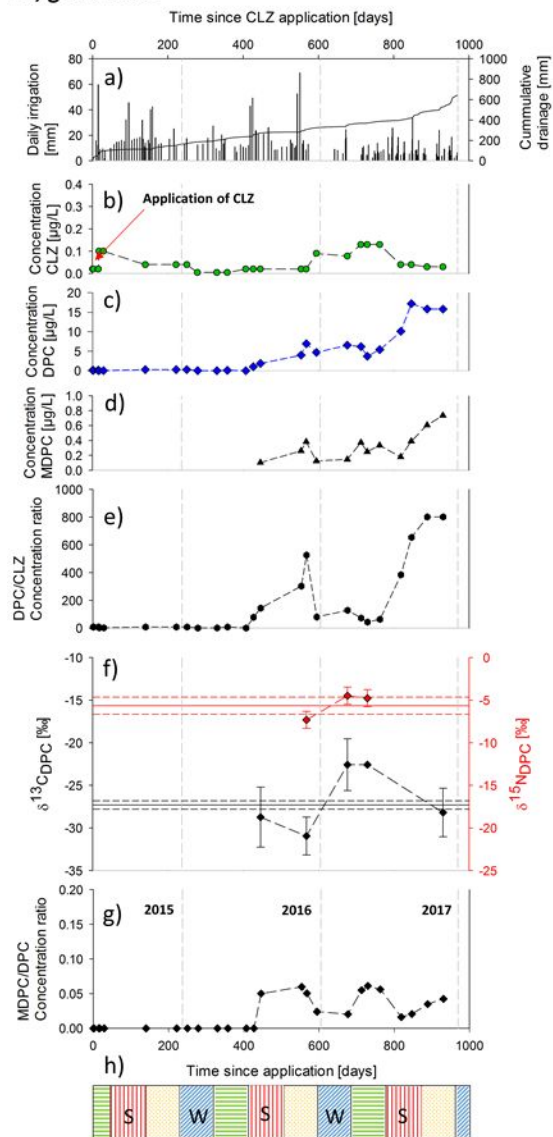
360

361 **CLZ Surface Application Mimicking A Realistic Field Scenario.** For the surface application of CLZ (Figure 2,
 362 L4 and L8), the metabolites DPC and MDPC were detected in the seepage water 425 days after CLZ
 363 application, coinciding with a heavy irrigation event (July 2016, Table S2), while the applied parent

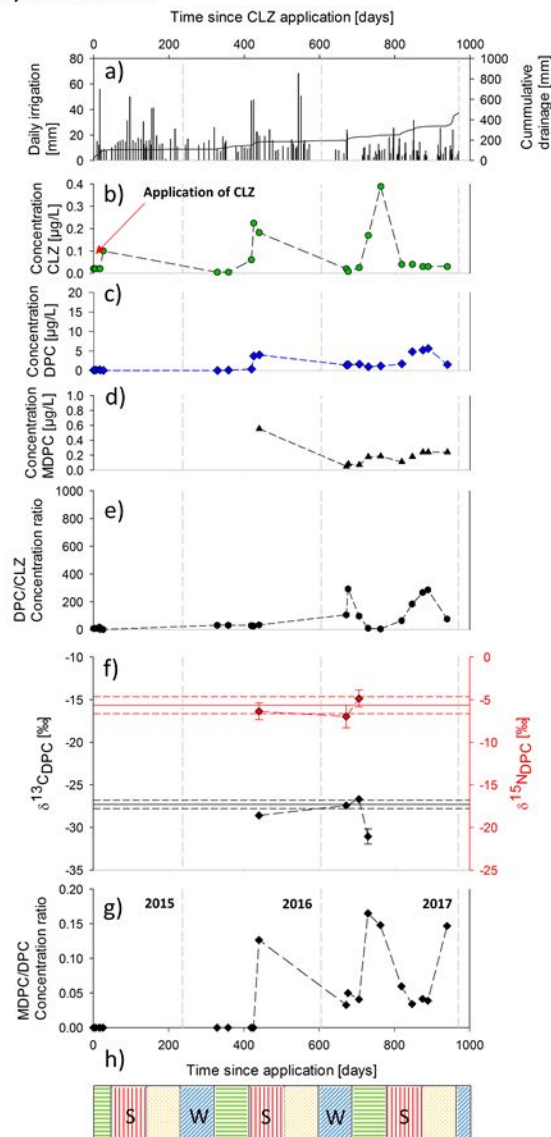
364 compound remained below or close to the limit of detection of 0.05 $\mu\text{g/L}$ during the time of monitoring
365 (970 days). Analytes breakthrough curves and concentrations differed between the soil types. For uranine,
366 a rapid breakthrough shortly after application was detected in moraine soil (Figure S4). During the
367 monitoring period, the maximum uranine concentration was measured within the first day, after only 4
368 mm of accumulated drainage (Table S6), suggesting that it was mainly transported through preferential
369 flow, bypassing large fractions of the soil matrix. Furthermore, a pronounced uranine peak tailing was
370 observed, which is typical for preferential flow (Figure S4). Furthermore, the DPC mass recovery curves
371 were significantly different for the two soils (Figure S5), giving further evidence of a greater contribution
372 of transport through preferential flow for moraine soil. This difference in soil type agrees with the results
373 of the lysimeters with surface application of DPC as well as well as with the findings for other compounds
374 described in Torrentó et al.³⁷.

375 Approximately 0.5 % and 0.13 % of the applied CLZ was leached as DPC after 950 days in gravel and
376 moraine soil, respectively. When analyzing the CLZ and DPC content in the upper soil, for none of the
377 lysimeters a closed mass balance was obtained. While no CLZ was detected in the first soil layer (0 to
378 10 cm) approximately 1 year after CLZ application to the lysimeter surface (consistent with Pestemer &
379 Malkomes⁴⁵), DPC amounts corresponding to 5 to 9 % of the applied CLZ were found (Table S7). CLZ and
380 DPC are expected to be incorporated into maize plants based on the findings of Schuhmann et al.⁴² and
381 Stephenson & Ries⁴³. In addition, Barra et al.⁴⁶ showed that during the first 90 days after CLZ application,
382 CLZ dissipation was mainly due to volatilization and degradation, whereas later on, when CLZ was already
383 in the subsurface, its disappearance from soil occurred mainly due to degradation. Higher DPC/CLZ
384 concentration values were measured in the drainage water of the gravel soil compared to moraine soil.
385 These results suggest that either DPC leached more rapidly through the soil matrix in the gravel soil
386 because of higher permeability. Or, alternatively, the extent of CLZ degradation was higher for the gravel
387 soil compared to moraine soil, as there is a greater contribution of preferential flow in moraine soil, which
388 bypasses the top layer where degradation is mostly expected to take place. When preferential flow occurs,
389 pesticides bypass large fractions of the soil matrix, reducing the degradation and sorption potential, as
390 the topsoil is microbiologically more active and with higher organic matter content. CSIA results provide
391 additional insights about these two hypotheses (see below). Concentration ratios and isotope results
392 point to a higher extent of CLZ degradation in gravel than in moraine soil. Nevertheless, some metabolite-
393 to-parent ratio values may be underestimated, because CLZ was below the limit of detection and,
394 therefore, CLZ concentrations corresponding to the detection limit were chosen for calculation, resulting
395 in a minimum estimated ratio in that case.

L4, gravel soil



L8, moraine soil



396

397 **Figure 2.** Lysimeters with CLZ application on surface (a single application in May 2015), L4 (left panels) and L8 (right panels). a)
 398 Daily irrigation (black bars) and cumulative drainage (grey line), b)-d) Concentration of CLZ (green circles), DPC (blue diamonds)
 399 and MDPC (black triangles) over time, e) metabolite-to-parent compound molar ratio of DPC/CLZ (black hexagon), f) carbon
 400 (black diamonds) and nitrogen (red diamonds) isotope ratios of DPC, error bars show the associated uncertainties (± 0.5 ‰ for
 401 carbon, ± 1.0 ‰ for nitrogen isotope analysis; or when exceeding this uncertainty, standard deviations of triplicate
 402 measurements are given, EA isotope values of the applied CLZ are shown as lines, whereas associated uncertainties (± 0.5 ‰
 403 for carbon, ± 1.0 ‰ for nitrogen isotope analysis) are shown as dashed lines in the corresponding color, respectively; g)
 404 metabolite-to-parent compound molar ratio of MDPC/DPC (black diamonds), h) season corresponding to the time since
 405 application – spring (green horizontal lines), summer (red vertical lines), autumn (yellow dots), winter (blue diagonal lines);
 406 the grey dashed lines repeated in each sub-figure represent the start of a new year.

407 In lysimeters with CLZ surface application (Figure 2, L4f and L8f), some carbon isotope values of DPC show
408 a shift to more negative $\delta^{13}\text{C}$ values compared to the carbon isotope signature of the applied CLZ (Table
409 S4). This behavior is observable in both lysimeters, especially after heavy rain events such as that one
410 performed 550 days after CLZ application (November 2016, Table S2), which resulted in a depletion in ^{13}C
411 by 3.4 ‰ for gravel soil (L4). This shift may be attributed to the mobilization of freshly formed DPC, which
412 is formed from CLZ by loss of the aromatic moiety through C–N bond cleavage. Presuming that the phenyl-
413 ring contains more ^{13}C atoms than the average molecule (Figure S1), which may have been introduced by
414 the synthesis process, this would result on a ^{13}C -depletion. Alternatively, the shift may be due to
415 secondary normal carbon isotope effects. Once transformation of DPC starts – as evidenced by the
416 detection of MDPC – this ^{13}C -depletion may be masked compared to the carbon isotope composition of
417 the applied CLZ, as an enrichment in ^{13}C in DPC is expected. Consistently, observed $\delta^{13}\text{C}_{\text{DPC}}$ values are close
418 to or higher than the EA-IRMS value of the applied CLZ.

419 In moraine soil (L8), no evidence of DPC degradation was obtained based on carbon isotope values, as
420 changes of $\delta^{13}\text{C}$ values were within the uncertainty of the method (Figure 2, L8f). In contrast, carbon
421 isotope values of DPC in gravel soil (L4) showed an enrichment in ^{13}C by up to +8.4 ‰ (Figure 2, L4f)
422 indicating that DPC was further transformed. At a subsequent time point (930 days after application),
423 however, the $\delta^{13}\text{C}_{\text{DPC}}$ value changed back close to the original isotopic signature detected at the beginning
424 of monitoring. This indicates that the change in $\delta^{13}\text{C}$ DPC values was “diluted” by the input of newly
425 mobilized DPC, as supported by a concomitant increase of the DPC/CLZ concentration ratio (Figure 2, L4e).
426 Hence, the two lines of evidence (isotope and DPC/CLZ concentration ratios) were found to complement
427 each other in the assessment of DPC degradation – when one line of evidence was about to fail, the other
428 was able to provide conclusive evidence.

429 The more substantial changes in both $\delta^{13}\text{C}_{\text{DPC}}$ values and DPC/CLZ concentration ratios indicate that DPC
430 degradation was higher in L4 (gravel soil) than in L8 (moraine soil) leading to the hypothesis that
431 differences in the transformation rate of CLZ to DPC existed. This is supported by the findings of Capri et
432 al.⁴⁷, who reported that the extent of CLZ degradation is influenced by the moisture content of the soil.
433 As described by Torrentó et al.³⁷, there is a higher soil water content and less fluctuation of the water
434 content in the gravel soil than in moraine soil. On the other hand, for both moraine and gravel soil, $\delta^{15}\text{N}$
435 values of the DPC formed are, as hypothesized in Figure S1, close to the nitrogen isotope signature of the
436 applied CLZ. Based on the findings of Lingens et al.²⁰, the pyridazinone-ring of the CLZ molecule is not
437 involved in the first transformation steps (dioxygenation of the phenyl-ring, Figure S1) so that no

438 significant nitrogen isotope fractionation is expected during CLZ transformation to DPC^{27, 29, 48, 49}. As the
439 isotope effect during multi-step reactions is reflected by the rate-limiting steps, our results indicate that
440 the amidase-driven cleavage of the moiety (2-hydroxymuconate) at the C–N bond, may be not rate-
441 limiting. As a result, changes in nitrogen isotope values of DPC can be uniquely attributed to its further
442 degradation.

443

444 **Transformation-Potential after Herbicide Injection Below the Root Zone.** Finally, two lysimeters (L6 and
445 L7) were chosen to simulate the preferential flow after a heavy irrigation event by injecting CLZ into a
446 depth of 40 cm, following the approach described by Torrentó et al.³⁷. In contrast to surface application
447 observations, CLZ and DPC broke through a few days after CLZ was injected (Figure S6). The second
448 metabolite MDPC was detected in the drainage water after 130 days. The detection of the metabolites
449 indicated that CLZ degradation occurred, even when it was injected below the root zone. Additionally,
450 significantly greater concentrations of CLZ, DPC and MDPC (1 to 2 orders of magnitude higher) were
451 measured in the drainage water of the lysimeter with CLZ depth injection compared to the CLZ surface
452 applications. In contrast to surface application observations, early breakthrough of injected uranine and
453 CLZ occurred for the two soil types within a few days (< 11 days for gravel and 6 hours for moraine soil)
454 and after a small amount of accumulated drainage (< 55 mm and 8 mm, respectively). This rapid response
455 and the peak tailing for both solutes are typical for preferential flow. More than 80 % of the total uranine
456 recovered mass was received during this early breakthrough. These results confirm that preferential flow
457 was enhanced by depth injection. In agreement with Torrentó et al.³⁷, the response to intense irrigation
458 events was more significant than for surface applications. It results in several fluctuations of CLZ and DPC
459 concentrations in the drainage water during the first 370 days for both soils (Figure S4). A great increase
460 in CLZ and DPC concentrations occurred in both lysimeters after 330-345 days (at 225-320 mm of
461 accumulated drainage), coinciding with the heavy irrigation events in May 2015 (Table S2). After this
462 pulse, no CLZ was recovered, while a steady increment in accumulated mass recovery was observed for
463 DPC for both soils (Figure S5).

464 At the end of the monitoring period (1250 days after CLZ injection), total leached analytes accounted for
465 24 and 22 % of the injected CLZ mass, respectively. Even though comparison between the two application
466 methods may be limited (eleven uniformly distributed CLZ injections versus broad surface application),
467 higher recoveries were obtained for CLZ injection after the same time of monitoring (950 days): from 2.0
468 to 3.4 % of CLZ, between 16.4 and 17.2 % of DPC and from 0.2 to 0.4 % of MDPC compared to no CLZ

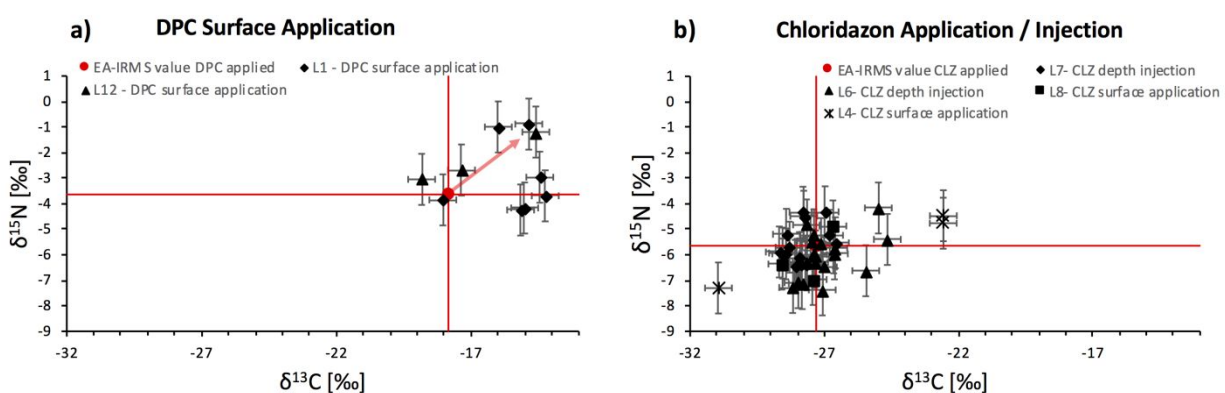
469 leaching, 0.13 to 0.15 % of DPC and below 0.02 % of MDPC with surface application. As the mass balance
470 remains incomplete for CLZ injection, there is evidence that additional processes occurred. With surface
471 application, processes such as volatilization⁴⁶, additional transformation pathways¹⁹ and uptake by
472 plants⁴² likely accounted for the mass losses. Additional influences on the low recovery, which might also
473 occur after CLZ depth injection, might be the low mobility for CLZ⁵⁰ and the formation of putative fulvic
474 acid complexes of DPC⁴⁴. The DPC/CLZ concentration ratio in these lysimeters with CLZ depth injection
475 shows that the main fraction of DPC seems not to be involved in sorption as this concentration ratio has
476 a single global maximum starting approximately 600 days after CLZ injection (Figure S6). This global
477 concentration maximum is two orders of magnitude greater than DPC/CLZ concentration ratios observed
478 for CLZ surface application. It shows the importance of the topsoil to retain DPC. As indicated by the
479 MDPC/DPC concentration ratio, further transformation of DPC occurred, although its extent and nature
480 is unknown.

481 ANOVA tests were performed to assess the differences between the two soil types and the CLZ application
482 method (i.e. surface application vs. depth injection) regarding DPC leaching and its carbon and nitrogen
483 isotope fractionation. The results showed that the DPC mass leached after 900 days was significantly
484 influenced by the CLZ application method ($p < 0.0001$). A 90- to 260-fold increase in DPC leaching was
485 observed for depth injection compared to surface application. Although the effect of soil type was not
486 statistically significant ($p = 0.998$), CLZ surface application resulted in higher DPC mass leached for gravel
487 than for moraine soil.

488 Similar to observations in lysimeters with CLZ surface application, carbon isotope data of DPC show an
489 enrichment in $\delta^{13}\text{C}$ of 3.8 ‰ after 648 days of herbicide injection below the root zone in the gravel soil,
490 while no significant change is observed in moraine soil (Figure S6). There, up to 648 days, no significant
491 changes in $^{13}\text{C}/^{12}\text{C}$ and $^{15}\text{N}/^{14}\text{N}$ ratios were measured. The $\delta^{15}\text{N}$ value of DPC shows the initial isotope
492 composition of the CLZ applied to the lysimeter. In very few cases, it was possible to measure $\delta^{15}\text{N}$ values
493 of MDPC formed from DPC (Figure S6 and Table S11). Nitrogen isotope values of MDPC were by
494 approximately 6 ‰ more negative than $\delta^{15}\text{N}$ signature of its parent compound DPC. This shift agrees with
495 the findings in DPC transformation experiments (Figure 1, L1 and L12) and, thus, supports the nitrogen
496 isotope effect of DPC methylation of approximately +12 ‰ as estimated above (Table S9 and S10).
497 According to the ANOVA results, isotope fractionation was mainly influenced by the soil type (higher ^{13}C
498 and ^{15}N enrichment for gravel soil) rather than by the CLZ application method.

499

500 **Dual-Element Isotope Plot to Identify DPC Formation and Transformation.** A dual-element plot was used
 501 for an overview of observed trends in carbon and nitrogen isotope signatures of DPC (i) either from
 502 formation from CLZ, or (ii) when DPC was further transformed. In Figure 3a, isotope data of all lysimeters
 503 with DPC surface application are combined, whereas in Figure 3b, data of all lysimeters with CLZ
 504 application/injection are shown. In Figure 3a, where DPC represents the original applied compound, a
 505 general trend towards more positive $\delta^{15}\text{N}$ and $\delta^{13}\text{C}$ values is observable. This observation is consistent
 506 with the well-established phenomenon that, in most cases, heavy isotopes become enriched in the
 507 remaining substrate during (bio)degradation. As detailed above, DPC in first drainage samples (first
 508 450 days) of the gravel soil showed a significant enrichment in ^{13}C but not in ^{15}N , indicating that two
 509 distinct processes for DPC transformation occurred. In contrast, Figure 3b shows two opposing trends
 510 pointing to the occurrence of both DPC formation and transformation. On the one hand, similar to the
 511 lysimeters with DPC application, a trend is observed towards more positive $\delta^{13}\text{C}$ and $\delta^{15}\text{N}$ values during
 512 the transformation of DPC. On the other hand, numerous data points show more negative $\delta^{13}\text{C}$ and $\delta^{15}\text{N}$
 513 isotope values. As this trend is only observable for lysimeters with CLZ application and injection, we
 514 attribute it to the formation of DPC. As discussed above, possible explanations for the observed depletion
 515 in ^{13}C (more negative $\delta^{13}\text{C}$ values) is (i) an artefact of an uneven ^{13}C isotope distribution in the cleaved
 516 phenyl-ring during DPC formation; or (ii) that the formation of DPC from CLZ (Figure S1) may be
 517 accompanied by a small and normal secondary carbon isotope effect.



518
 519 **Figure 3.** Dual-element isotope plot of a) DPC degradation in lysimeters L1 and L12, where DPC was applied on the surface, and
 520 b) formation and degradation of DPC in the lysimeters where CLZ was either applied (L4 and L8) or injected in a depth of 40 cm
 521 (L6 and L7); the red circles represent the isotopic signature of the applied/injected a) DPC and b) CLZ – position of CLZ and DPC
 522 differ within the dual-element isotope plots due to their different isotopic source signatures (Table S4).

523

524 **Environmental Significance and Outlook**

525 The isotope fractionation in DPC observed for the three tested scenarios is particularly important because
526 (i) the change in carbon and nitrogen isotopic signature of DPC evidenced transformation of an apparently
527 persistent metabolite, and (ii) these changes provide evidence that likely more than one transformation
528 pathway is involved in DPC transformation. In soil, only methylation of DPC to MDPC is known and thus
529 our data suggest the need for further laboratory experiments and mechanistic studies on DPC
530 (bio)degradation to gain further insight into possible additional transformation pathways. (iii) Formed
531 DPC, which had not been subject to further transformation yet, showed the same nitrogen isotope
532 signature as its precursor CLZ. Hence, $\delta^{15}\text{N}$ values may serve as isotopic fingerprints to identify the origin
533 of such compounds in groundwater.

534 When applying CSIA, the combination with conventional methods was found to be complementary and
535 advantageous, especially when formation and transformation of the metabolite was occurring
536 simultaneously. Once introduction of newly formed metabolite dominated, evidence from CSIA was not
537 necessarily conclusive because transformation-related changes in isotope ratios were masked by the
538 continuous input of DPC. Here, additional information was gained by metabolite-to-parent concentration
539 ratios, which became greatest and could provide evidence of DPC formation. Vice versa, when metabolite-
540 to-parent-ratios were small because DPC was further transformed, it was the changes in isotope ratios of
541 DPC which still carried the isotopic imprint of the reaction and, hence, made transformation visible. For
542 further understanding of the environmental fate of DPC, reference experiments focusing on the
543 determination of stable isotope fractionation factors as well as microbial processes during DPC
544 transformation are required in order to identify transformation mechanisms and quantify them.

545 For the future, our approach with CSIA in combination with concentration measurements and systematic
546 long-term lysimeter experiments holds promise to answer questions about transformation pathways and
547 the extent of soil / vadose zone (bio)transformation not only for DPC – one of the most widely detected
548 substances – in groundwater, but also for other micropollutants of concern and their metabolites.
549 Additionally, this study confirmed that the application of CSIA in combination with solid-phase
550 extraction^{27, 39} is feasible for the analysis of polar micropollutants in drainage water at environmentally
551 relevant concentrations. Thus, it can be also applied to studies in agricultural soil and groundwater from
552 common unconsolidated sand and/or gravel aquifers with catchment areas within agricultural production.

553 **ASSOCIATED CONTENT**

554 *** Supporting Information**

555 Further details on chemicals, lysimeters, analytical methods, analyte recovery calculations and results of
556 water balance computation, vegetation cover evolution, breakthrough trends, EA-IRMS analyses, soil
557 analyses, CLZ depth injection and nitrogen isotope ratios.

558

559 **AUTHOR INFORMATION**

560 **Corresponding Author**

561 *Phone: + 49 89 2180 78232; fax: + 49 89 2180 78255; e-mail: m.elsner@tum.de

562

563 **Author Contributions**

564 [∇]These authors contributed equally as first authors to this work.

565 **Present Addresses**

566 [§]Technical University of Munich, Chair of Analytical Chemistry and Water Chemistry, 81377 Munich,
567 Germany.

568 [†]Grup MAiMA, Departament de Mineralogia, Petrologia i Geologia Aplicada, Facultat de Ciències de la
569 Terra, Universitat de Barcelona (UB), C/ Martí i Franquès s/n, 08028, Barcelona, Spain.

570 [¶]Département des sciences de la Terre et de l'atmosphère, Université du Québec à Montréal, 201 avenue
571 du Président Kennedy, Montréal, QC, Canada.

572 **Notes**

573 The authors declare no competing financial interest.

574 **ACKNOWLEDGMENT**

575 This study was supported by the project CRSII2_141805/1 from the Swiss National Science Foundation
576 (SNSF). The authors would like to thank the NPAC (UNiNE) and Jakov Bolotin (Eawag) for their help in the
577 laboratory as well as Doris Ebert from BASF for providing the chemical DPC.

578

579 **ABBREVIATIONS**

580 CLZ - 5-Amino-4-chloro-2-phenyl-2*H*-pyridazin-3-one

581 DPC - 5-Amino-4-chloro-3(2*H*)-pyridazinone

582 MDPC - 5-Amino-4-chloro-2-methyl-3(2*H*)-pyridazinone

583

584 **References**

- 585 1. European Commission, Groundwater Protection in Europe The new Groundwater Directive:
586 consolidating the EU regulatory framework In *European Commission-Directorate-General for*
587 *Environment*, EU Publications: Brussels, 2008.
- 588 2. BAFU, B. f. U., Pflanzenschutzmittel PSM und PSM-Abbauprodukte im Grundwasser. In NAQUA,
589 N. G., Ed. Switzerland, 2013.
- 590 3. Loos, R.; Gawlik, B. M.; Locoro, G.; Rimaviciute, E.; Contini, S.; Bidoglio, G., EU-wide survey of
591 polar organic persistent pollutants in European river waters. *Environ. Pollut.* **2009**, *157*, (2), 561-568.
- 592 4. Reemtsma, T.; Alder, L.; Banasiak, U., A multimethod for the determination of 150 pesticide
593 metabolites in surface water and groundwater using direct injection liquid chromatography–mass
594 spectrometry. *J. Chromatogr. A* **2013**, *1271*, (1), 95-104.
- 595 5. Postigo, C.; Barceló, D., Synthetic organic compounds and their transformation products in
596 groundwater: Occurrence, fate and mitigation. *Sci. Total Environ.* **2015**, *503–504*, 32-47.
- 597 6. Fenner, K.; Canonica, S.; Wackett, L. P.; Elsner, M., Evaluating Pesticide Degradation in the
598 Environment: Blind Spots and Emerging Opportunities. *Science* **2013**, *341*, (6147), 752-758.
- 599 7. Thier, H.-P.; Zeumer, H., *Manual of Pesticide Residue Analysis Volume I*. VCH Verlagsgesellschaft:
600 1987; p 443.
- 601 8. Drescher, N.; Otto, S., Über den Abbau von 1-Pheny1-4-amino-5-chlor-pyridazon-6 (Pyrazon) im
602 Boden *Zeitschrift für Pflanzenkrankheiten (Pflanzenpathologie) und Pflanzenschutz* **1969**, *76*, (1), 27-33.
- 603 9. Hertfordshire, U. o., PPDB: Pesticide Properties DataBase. In University of Hertfordshire:
604 <http://sitem.herts.ac.uk/aeru/ppdb/en/Reports/141.htm>, 2018.
- 605 10. Buttiglieri, G.; Peschka, M.; Frömel, T.; Müller, J.; Malpei, F.; Seel, P.; Knepper, T. P.,
606 Environmental occurrence and degradation of the herbicide n-chloridazon. *Water Res.* **2009**, *43*, (11),
607 2865-2873.
- 608 11. Loos, R.; Locoro, G.; Comero, S.; Contini, S.; Schwesig, D.; Werres, F.; Balsaa, P.; Gans, O.; Weiss,
609 S.; Blaha, L.; Bolchi, M.; Gawlik, B. M., Pan-European survey on the occurrence of selected polar organic
610 persistent pollutants in ground water. *Water Res.* **2010**, *44*, (14), 4115-4126.
- 611 12. Weber, W. H.; Seitz, W.; Schulz, W.; Wagener, H.-A., Nachweis der Metaboliten Desphenyl-
612 chloridazon und Methyl-desphenyl-chloridazon in Oberflächen, Grund- und Trinkwasser. *Vom Wasser*
613 **2007**, *105* (1), 7-14.
- 614 13. Reinhardt, M. K., Ronald; Hofacker, Anke; Leu, Christian Monitoring von PSM-Rückständen im
615 Grundwasser. *Aqua Gas* **2017**, *6*, 78-89.
- 616 14. Sturm, S.; Kiefer, J.; Kollotzek, D.; Rogg, J.-m., Aktuelle Befunde der Metaboliten von Tolyfluanid
617 und Chloridazon in den zur Trinkwasserversorgung genutzten Grundwasservorkommen Baden-
618 Württembergs. *gwf Wasser | Abwasser* **2013**, (10), 950-959%V 151.
- 619 15. Deutsche-Forschungsgemeinschaft, *Rückstandsanalytik von Pflanzenschutzmitteln“, Mitteilung*
620 *VI der Senatskommission für Pflanzenschutz-, Pflanzenbehandlungs- und Vorratsschutzmittel,*
621 *Methodensammlung der Arbeitsgruppe Analytik, 11*. Wiley VCH: 1990.
- 622 16. Gustafson, D. I., Groundwater ubiquity score: A simple method for assessing pesticide
623 leachability. *Environmental Toxicology and Chemistry* **1989**, *8*, (4), 339-357.
- 624 17. Grummt, T. P., Rudolf, Gesundheitliche Orientierungswerte (GOW) für nicht relevante
625 Metaboliten (nrM) von Wirkstoffen aus Pflanzenschutzmitteln (PSM). In Risikobewertung, U. a. B. f., Ed.
626 Umweltbundesamt and Bundesinstitut für Risikobewertung:
627 <https://www.umweltbundesamt.de/dokument/gesundheitsliche-orientierungswerte-gow-fuer-nicht>,
628 2017; p 12.
- 629 18. UBA, Pflanzenschutzmittelfunde im Grundwasser. In Umweltbundesamt: 2004.

- 630 19. Roberts, M. C.; Croucher, L.; Roberts, T. R.; Hutson, D. H.; Lee, P. W.; Nicholls, P. H.; Plimmer, J.
631 R., *Metabolic Pathways of Agrochemicals: Part 1: Herbicides and Plant Growth Regulators*. Royal Society
632 of Chemistry: 2007.
- 633 20. Lingens, F.; Blecher, R.; Blecher, H.; Blobel, F.; Eberspächer, J.; Fröhner, C.; Görisch, H.; Görisch,
634 H.; Layh, G., *Phenylobacterium immobile* gen. nov., sp. nov., a Gram-Negative Bacterium That Degrades
635 the Herbicide Chloridazon. *Int. J. Syst. Evol. Microbiol.* **1985**, *35*, (1), 26-39.
- 636 21. Farlin, J.; Bayerle, M.; Pittois, D.; Gallé, T., Estimating Pesticide Attenuation From Water Dating
637 and the Ratio of Metabolite to Parent Compound. *Groundwater* **2017**, *55*, (4), 550-557.
- 638 22. Meyer, A. H.; Elsner, M., 13C/12C and 15N/14N Isotope Analysis To Characterize Degradation of
639 Atrazine: Evidence from Parent and Daughter Compound Values. *Environ. Sci. Technol.* **2013**, *47*, (13),
640 6884-6891.
- 641 23. Hunkeler, D.; Meckenstock, R. U.; Sherwood Lollar, B.; Schmidt, T.; Wilson, J.; Schmidt, T.;
642 Wilson, J. *A Guide for Assessing Biodegradation and Source Identification of Organic Ground Water*
643 *Contaminants using Compound Specific Isotope Analysis (CSIA)*; PA 600/R-08/148 | December 2008 |
644 www.epa.gov/ada; US EPA: Oklahoma, USA, 2008.
- 645 24. Thullner, M.; Richnow, H.-H.; Fischer, A., Characterization and quantification of *in situ*
646 biodegradation of groundwater contaminants using stable isotope fractionation analysis: advantages
647 and limitations. In *Environmental and Regional Air Pollution*, Gallo, D.; Mancini, R., Eds. Nova Science
648 Publishers: 2009.
- 649 25. Meckenstock, R. U.; Morasch, B.; Griebler, C.; Richnow, H. H., Stable isotope fractionation
650 analysis as a tool to monitor biodegradation in contaminated aquifers. *Journal of Contaminant*
651 *Hydrology* **2004**, *75*, (3-4), 215-255.
- 652 26. Alvarez-Zaldívar, P.; Payraudeau, S.; Meite, F.; Masbou, J.; Imfeld, G., Pesticide degradation and
653 export losses at the catchment scale: Insights from compound-specific isotope analysis (CSIA). *Water*
654 *Res.* **2018**, *139*, 198-207.
- 655 27. Melsbach, A.; Ponsin, V.; Torrentó, C.; Lihl, C.; Hofstetter, T. B.; Hunkeler, D.; Elsner, M., 13C and
656 15N isotope analysis of desphenylchloridazon by liquid chromatography isotope ratio mass
657 spectrometry (LC-IRMS) and derivatization-gas chromatography isotope ratio mass spectrometry (GC-
658 IRMS). *Anal. Chem.* **2019**, *91*, (5), 3412-3420.
- 659 28. Elsner, M., Stable isotope fractionation to investigate natural transformation mechanisms of
660 organic contaminants: principles, prospects and limitations. *J. Environ. Monit.* **2010**, *12*, (11), 2005-2031.
- 661 29. Muller, R.; Schmitt, S.; Lingens, F., A novel non-heme iron-containing dioxygenase. Chloridazon-
662 catechol dioxygenase from *Phenylobacterium immobilis* DSM 1986. *European journal of biochemistry /*
663 *FEBS* **1982**, *125*, (3), 579-84.
- 664 30. Braeckevelt, M.; Fischer, A.; Kästner, M., Field applicability of Compound-Specific Isotope
665 Analysis (CSIA) for characterization and quantification of *in situ* contaminant degradation in aquifers.
666 *Appl. Microbiol. Biotechnol.* **2012**, *94*, (6), 1401-1421.
- 667 31. Kopinke, F. D.; Georgi, A.; Voskamp, M.; Richnow, H. H., Carbon isotope fractionation of organic
668 contaminants due to retardation on humic substances: Implications for natural attenuation studies in
669 aquifers. *Environ. Sci. Technol.* **2005**, *39*, (16), 6052-6062.
- 670 32. Fischer, A.; Theuerkorn, K.; Stelzer, N.; Gehre, M.; Thullner, M.; Richnow, H. H., Applicability of
671 Stable Isotope Fractionation Analysis for the Characterization of Benzene Biodegradation in a BTEX-
672 contaminated Aquifer. *Environ. Sci. Technol.* **2007**, *41*, (10), 3689-3696.
- 673 33. Morrill, P. L.; Sleep, B. E.; Seepersad, D. J.; McMaster, M. L.; Hood, E. D.; LeBron, C.; Major, D.
674 W.; Edwards, E. A.; Sherwood Lollar, B., Variations in expression of carbon isotope fractionation of
675 chlorinated ethenes during biologically enhanced PCE dissolution close to a source zone. *Journal of*
676 *Contaminant Hydrology* **2009**, *110*, (1-2), 60-71.

- 677 34. Stehmeier, L. G.; Francis, M. M.; Jack, T. R.; Diegor, E.; Winsor, L.; Abrajano, T. A., Field and in
678 vitro evidence for in-situ bioremediation using compound-specific $^{13}\text{C}/^{12}\text{C}$ ratio monitoring. *Org.*
679 *Geochem.* **1999**, *30*, (8, Part 1), 821-833.
- 680 35. Hunkeler, D.; Aravena, R.; Parker, B. L.; Cherry, J. A.; Diao, X., Monitoring oxidation of
681 chlorinated ethenes by permanganate in groundwater using stable isotopes: laboratory and field
682 studies. *Environ. Sci. Technol.* **2003**, *37*, 798-804.
- 683 36. Elsner, M.; Lacrampe Couloume, G.; Mancini, S. A.; Burns, L.; Sherwood Lollar, B., Carbon
684 Isotope Analysis to Evaluate Nanoscale Fe(0) Treatment at a Chlorohydrocarbon Contaminated Site.
685 *Groundwater Monitoring and Remediation* **2010**, *30*, 79-95.
- 686 37. Torrentó, C.; Prasuhn, V.; Spiess, E.; Ponsin, V.; Melsbach, A.; Lihl, C.; Glauser, G.; Hofstetter, T.
687 B.; Elsner, M.; Hunkeler, D., Adsorbing vs. Nonadsorbing Tracers for Assessing Pesticide Transport in
688 Arable Soils. *Vadose Zone J.* **2018**, *17*, (1).
- 689 38. IUSS_Working_Group_WRB, *World Reference Base for Soil Resources 2014, update 2015 -*
690 *International soil classification system for naming soils and creating legends for soil maps.* . Food and
691 Agriculture Organization of the United Nations: Rome, 2015; Vol. 106.
- 692 39. Torrentó, C.; Bakkour, R.; Gaétan, G.; Melsbach, A.; Ponsin, V.; Hofstetter, T. B.; Elsner, M.;
693 Hunkeler, D., Solid-phase extraction method for stable isotope analysis of pesticides from large volume
694 environmental water samples. *Analyst* **2019**, *144*, (9), 2898-2908
- 695 40. Meyer, A. H.; Penning, H.; Lowag, H.; Elsner, M., Precise and accurate compound specific carbon
696 and nitrogen isotope analysis of atrazine: critical role of combustion oven conditions. *Environ. Sci.*
697 *Technol.* **2008**, *42*, (21), 7757-7763.
- 698 41. Werner, R. A.; Brand, W. A., Referencing strategies and techniques in stable isotope ratio
699 analysis. *Rapid Commun. Mass Spectrom.* **2001**, *15*, 501-519.
- 700 42. Schuhmann, A.; Gans, O.; Weiss, S.; Fank, J.; Klammler, G.; Haberhauer, G.; Gerzabek, M., A long-
701 term lysimeter experiment to investigate the environmental dispersion of the herbicide chloridazon and
702 its metabolites—comparison of lysimeter types. *J. Soils Sediments* **2016**, *16*, (3), 1032-1045.
- 703 43. Stephenson, G. R.; Ries, S. K., Metabolism of Pyrazon in Sugar Beets and Soil. *Weed Science*
704 **1969**, *17*, (3), 327-331.
- 705 44. Gatzweiler, E., Das Langzeitverhalten der Herbizidwirkstoffe Chloridazon und 2, 4-DP-P nach
706 Praxisanwendung in zwei verschiedenen Boden der Bundesrepublik. **1993**.
- 707 45. PESTEMER, W.; MALKOMES, H.-P., Einfluss von Pflanzenschutzmitteln einer Zuckerrüben-
708 Spritzfolge auf biologische Aktivitäten und auf den Abbau von Chloridazon im Boden. I.
709 Freilandversuche. *Weed Res.* **1983**, *23*, (5), 283-291.
- 710 46. Barra, R.; Vighi, M.; Di Guardo, A., Prediction of surface water input of chloridazon and
711 chlorpyrifos from an agricultural watershed in Chile. *Chemosphere* **1995**, *30*, (3), 485-500.
- 712 47. Capri, E.; Ghebbioni, C.; Trevisan, M., Metamitron and Chloridazon Dissipation in a Silty Clay
713 Loam Soil. *J. Agric. Food Chem.* **1995**, *43*, (1), 247-253.
- 714 48. Elsner, M.; Zwank, L.; Hunkeler, D.; Schwarzenbach, R. P., A new concept linking observable
715 stable isotope fractionation to transformation pathways of organic pollutants. *Environ. Sci. Technol.*
716 **2005**, *39*, (18), 6896-6916.
- 717 49. Elsner, M.; Jochmann, M. A.; Hofstetter, T. B.; Hunkeler, D.; Bernstein, A.; Schmidt, T. C.;
718 Schimmelmann, A., Current challenges in compound-specific stable isotope analysis of environmental
719 organic contaminants. *Anal. Bioanal. Chem.* **2012**, *403*, (9), 2471-2491.
- 720 50. DE FANG, F.; PESTEMER, W.; MALKOMES, H.-P., Einfluss von Pflanzenschutzmitteln einer
721 Zuckerrüben-Spritzfolge auf biologische Aktivitäten und auf den Abbau von Chloridazon im Boden. II.
722 Gefäß- und Laborversuche. *Weed Res.* **1983**, *23*, (5), 293-304.

723